HHS Public Access

Author manuscript

Acta Biomater. Author manuscript; available in PMC 2017 March 01.

Published in final edited form as:

Acta Biomater. 2016 March 1; 32: 223–230. doi:10.1016/j.actbio.2015.12.031.

Myofibroblast Persistence with Real-Time Changes in Boundary Stiffness

Mehmet H. Kural and **Kristen L. Billiar**

Department of Biomedical Engineering, Worcester Polytechnic Institute, Worcester, MA, USA

Abstract

Myofibroblasts are critical for connective tissue remodeling and wound healing since they can close wound beds and shape tissues rapidly by generating high traction forces and secreting abundant extracellular matrix proteins and matrix metalloproteinases. However, their presence in excessive numbers is associated with fibrotic and calcific diseases and tissue thickening in engineered tissues. While activation of the myofibroblast phenotype has been studied extensively, whether myofibroblasts are “cleared” by phenotypic reversal or by apoptosis remains controversial. The goal of this work is to test the hypothesis that mechanical inhibition of myofibroblast force generation leads to de-differentiation or apoptosis depending upon the magnitude of the decrease in tension. To test this hypothesis, we cultured valvular interstitial cells (VICs) in fibrin micro-tissues suspended between flexible posts and dynamically altered the ability of the cells to generate tension by altering boundary stiffness via magnetic forces applied to posts. The flexible posts capped with magnetic beads enable the measurement and modulation of tension generated by the cells within the tissue. As expected, the cell-generated forces were elevated with dynamically increased boundary (post) stiffness, yet surprisingly, the forces continued to increase following dynamic reduction of boundary stiffness back to baseline levels. Increased apoptosis and reduced α-SMA staining were observed with complete freeing of the tissues from the posts but not upon removal of the magnet, resulting in a two-fold decrease in post stiffness. Together, these data indicate that an increase in myofibroblast force generation, even if modest and temporary (1 day), can have lasting effects on myofibroblast persistence in tissues, and that a significant reduction in the ability of the cells to generate tension is required to trigger dedifferentiation and/or apoptosis. The ability to dedifferentiate myofibroblasts to a quiescent phenotype and to control the percentage of apoptosis would be of great benefit for therapeutic and tissue engineering applications.

Graphical abstract

Address for Correspondence: Kristen L. Billiar, Ph.D., Professor, Department of Biomedical Engineering, Worcester Polytechnic Institute, 100 Institute Road, Worcester, MA 01609, Tel: 508-831-5384, Fax: 508-831-5541, kbilliar@wpi.edu.

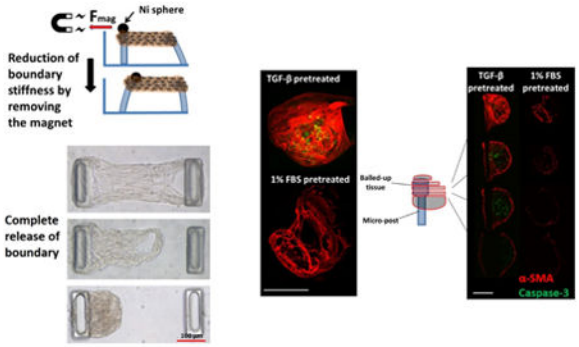

Keywords

Valvular interstitial cell; myofibroblast; stiffness; tension; fibrin; three-dimensional; TGF-β1; apoptosis; mechanobiology

1. Introduction

Myofibroblasts play a key role in tissue remodeling and wound healing [1, 2]. Being able to generate high traction forces and secrete abundant extracellular matrix (ECM) proteins, myofibroblasts can reorganize their surrounding matrix, rapidly close wounds and repair matrix damage [3]. However, prolonged presence of myofibroblasts due to excessive activation of fibroblasts and/or insufficient myofibroblast apoptosis leads to fibrocontractive remodeling and scar tissue [3-5]. By compacting the surrounding matrix, digesting native ECM and secreting excessive amounts of stiff collagen under high residual tension, myofibroblasts contribute to diseas states of many different organs [6-8].

In heart valves, activation of a large proportion of valvular interstitial cells (VICs) to the myofibroblast phenotype is associated with valve fibrosis which may cause regurgitation, valve failure [9]. Moreover, in over 80% of calcified aortic valves, myofibroblasts are colocalized with the calcified regions and apoptotic cells [9]. In addition to being associated with disease of native heart valves, myofibroblasts are responsible for tissue thickening and retraction in engineered heart valves [10, 11]. Thus, being able to reverse the myofibroblast phenotype (i.e., dedifferentiate VICs back to the quiescent state) and/or control the rate of clearing of myofibroblasts from the tissue via apoptosis would be of great benefit for therapeutic applications.

High substrate modulus and transforming growth factor-beta1 (TGF-β1) have been shown to be key activators of fibroblasts and VICs to the myofibroblast phenotype [12-14]. Specifically, on high modulus substrates in the presence of TGF-β1, fibroblastic cells form α-SMA-rich stress fibers – the defining visual hallmark of the myofibroblast phenotype – and generate high intracellular tension. We recently demonstrated quantitatively that this synergistic relationship between stiffness and TGF-β1 in modulating VIC-generated forces also applies to three-dimensional (3D) tissue models [15].

Although, the mechanical environment is clearly critical for triggering myofibroblast activation, little is known about the mechanical reversibility of this phenotype. Early *in vivo*

data indicated that myofibroblasts are cleared following wound closure by apoptosis (i.e., programmed cell death) rather than by dedifferentiation [16]. Externally reducing the resistance to cell contraction has also been shown to trigger apoptosis; for example, releasing a stiff splint holding the edges of an excisional wound caused apoptosis in 8% of the total cell population [17]. In an analogous *in vitro* 3D system in which collagen gels seeded with dermal myofibroblasts were detached from rigid boundaries, apoptosis was triggered in 15% of the cells [18]. A similar study utilizing fibroblasts isolated from scar tissue [19] reported 40% apoptosis following the release of anchored collagen gels.

More recently, however, there is evidence that myofibroblasts may dedifferentiate without apoptosis in response to changes in the mechanical environment. Hinz and colleagues showed that α-SMA expression in dermal fibroblasts decreases without apoptosis when a splinted wound bed is released [20]. Anseth and her group seeded VICs on light-responsive gel substrates for three days, then dynamically decreased the Young's modulus of the gel [21, 22]. They observed a significant decrease in the number of cells expressing α-SMA without inducing apoptosis above the level of stiffness-matched controls, thus indicating phenotypic reversion after two additional days of culture at the lower modulus. However, when they cultured VICs on stiff gels for a longer time period (seven days), reduction of substrate modulus did not result in dedifferentiation [22]. In the aforementioned 2D and 3D studies, the experimental manipulations reduce the mechanical restraints to cell-generated tension, but in none of the studies is the tension quantified; thus it is unclear if the magnitude of tension is a key parameter for differentially regulating dedifferentiation and/or apoptosis.

The goal of this work is to test the hypothesis that mechanical inhibition of myofibroblast force generation leads to either dedifferentiation or apoptosis, depending upon the magnitude of the decrease in intracellular tension. To test this hypothesis, we cultured VICs in 3D fibrin micro-tissues suspended between flexible posts, the deflection of which can be used to quantify the tissue tension. To determine the effect of mechanical tension drop on the myofibroblast phenotype, we stimulated cell-generated forces by doubling the boundary stiffness in real time by holding one of the micro-posts rigid via magnetic force applied to a nickel bead glued onto the post; the post was then released by removing the permanent magnet. To create a more severe tension drop, we released tissues completely from one of the micro-posts and cultured the tissues without constraining contraction towards the remaining micro-post. The findings of the present study provide insight for future studies aimed at directing myofibroblast fate in in both diseased and engineered tissues.

2. Methods

2.1 Cell Culture

Pig hearts were obtained from a local slaughterhouse (Blood Farm, Groton, MA). Aortic valves were excised within two hours after animals were killed. VICs were isolated according to a previously published protocol [23]. Aortic valve leaflets were rinsed with cold 1× Dulbecco's phosphate buffered saline (DPBS, Cellgro, Manassas, VA), and submerged in a 600 U/mL solution of type II collagenase (Worthington Biochemical, Lakewood, NJ) in 1× Dulbecco's Modified Eagle's Medium (DMEM, ThermoFisher, Grand

Island, New York) with 1% penicillin / streptomycin / amphotericin B (PSA, Life Technologies, Grand Island, New York) and 10% fetal bovine serum (FBS, Life Technologies, Grand Island, New York). Both surfaces of the leaflets were rubbed by a sterile cotton swab to remove the valvular endothelial cells in a collagenase solution. Next, the leaflets were rinsed and incubated in 12 ml of collagenase solution at 37°C for 12 hours for enzymatic digestion. Finally, VICs were plated on tissue culture plastic flasks in DMEM with 1% PSA and 10% FBS. Cell passage numbers 3 to 8 were used. Two types of pre-treatments were utilized in the current study as follows: the first group was pre-treated with low serum media containing 1% FBS without TGF-β1 for four days to have a more quiescent population with lower tissue tension (low tension group), and the second group was pre-treated with 10% FBS and 5 ng/ml TGF-β1 for four days to activate all cells to a myofibroblast phenotype (high tension group) as per [18].

2.2 Force Calculations with Micro-tissue Gauges (μ-TUGs)

We utilized fibrin gels as our 3D scaffold (rather than collagen) due to the high efficiency of creating micro-tissues that could be cultured for long duration. In addition to its technical advantage, fibrin is abundant in damaged heart valve tissue, and it is extensively used in tissue engineered heart valve studies since fibrin gels, unlike reconstituted collagen gels, do not inhibit collagen production by the resident cells [10, 24]. As we described previously [15], to measure and regulate cell-generated forces, fibrin-based micro-tissues were cultured in micro-wells containing two flexible posts made of poly(dimethylsiloxane) (PDMS, Dow Corning, Midland, MI). As cells compact the fibrin gel and form dog-bone shaped tissues around the posts, the forces applied to the posts can be calculated by measuring the posts' deflection and using the following beam bending equations: $=\frac{wt^3}{12}$ and $\boldsymbol{F}=\frac{\delta * 6EI}{a^2 * (3L-a)}$, where δ is the post deflection and all the other parameters are dimensional parameters shown in Figure 1.

Post deflections were measured at multiple time points and under various boundary conditions; in general, they were measured immediately before and after applying the magnet, ∼10 hours following applying the magnet, immediately before removing magnet, immediately after removing the magnet, 12 hours after removing the magnet, and two days after removing the magnet. The post held rigidly by the applied magnetic force acts as an infinitely stiff boundary which causes a doubling of the effective boundary stiffness as explained in the next sections. The average force per cell was calculated by dividing the total force applied to one of the posts by the average number of representative volume elements (RVEs) spanning a cross-sectional area in the middle of the micro-tissue [15].

2.3 VIC-Populated Fibrin Micro-Tissues

Empty μ-TUG wells were treated with 3.5% Pluronic F-127 (Invitrogen, Eugene, Oregon) to prevent cell attachment to the PDMS. VICs were re-suspended in fibrin gel solution [final concentration 160,000 cell/ml, 3.3 mg/ml fibrinogen from bovine plasma (Sigma, St. Louis, MO) and 0.22 U/ml thrombin (Sigma, St. Louis, MO)]. The cell−gel mixture was centrifuged in the micro wells, and the excess gel solution remaining was aspirated out of the wells. Following a one-hour incubation at 37°C to allow gel polymerization, culture

medium containing DMEM with 1% PSA, 33.3 μg/ml aprotinin (Sigma, St. Louis, MO) and 50 μg/ml L-ascorbic acid phosphate magnesium salt N-hydrate was added to μ-TUG wells with either 10% FBS and 1 ng/ml TGF-(β1 (high tension group) or 1% FBS with no TGF-(β1 (low tension group). Supplementation with 1 ng/ml TGF-(β1 and 10% FBS was chosen to culture micro-tissues in the high tension group since it gives the maximal tension change by softening the boundary as described in the next section. Different micro-post stiffness levels were obtained by using different PDMS monomer-to-curing agent ratios and different baking temperatures as described previously [15].

2.4 Changing Boundary Stiffness in Real Time

The tension in the micro-tissues created by cell-generated forces is transferred via other cells and the ECM to the boundaries (the flexible posts in our system). Reciprocally, the bending stiffness of the posts is transduced by the cells as it alters the overall deformation of the tissue, which occurs due to a given level of cell-generated tension. When the tissues are suspended between two flexible posts, the effective (resultant) boundary stiffness can be calculated as $k_{eff}^{-1}=k_1^{-1}+k_2^{-1}$ as per two springs in series. To dynamically double the boundary stiffness, one of the micro-posts in each well was held rigidly by applying magnetic force to a nickel sphere (Alfa Aesar, 200 mesh diameter = 100-150 μm, Ward Hill, Massachusetts) glued on top of the post as shown in Figure 2. As shown in Figure 2-B, for two identical posts, holding one of the posts rigidly (i.e., infinite stiffness) doubles the effective boundary stiffness. We performed initial studies to optimize the conditions to obtain a maximal tension drop upon removal of the magnetic force (reduction of boundary stiffness in real time). To determine the experimental conditions that would provide the maximum cell response to a change in boundary stiffness, we used our previously generated response surface of cell-generated forces as a function of boundary stiffness and TGF-β1 concentration to choose regions with high gradients in force with respect to stiffness [15]. Micro-posts with individual stiffness of 0.33 nN/nm ($k_{eff} = k_{post}/2 = 0.165$ nN/nm) were chosen as the low boundary stiffness level since, at this level, cell-generated forces remain constant after two days, whereas at 0.56 nN/nm stiffness ($k_{eff} = 0.28$ nN/nm), the forces continue to increase for seven days when cultured in the presence of TGF-β1 (Supplementary Fig.1) [15]. Therefore, dynamically increasing the effective boundary stiffness in real time from $k_{eff} = 0.165$ nN/nm to $k_{eff} = 0.33$ nN/nm by holding one post rigidly (Figure 2-B) was expected to provide a transition between the two phenotypic states (Supplementary Fig. 1). Data regarding the optimization trials necessary to maximize the change in tension with dynamically altered boundary stiffness are provided as supplemental data (Supplementary Fig. 2 and 3). Following one day of fibrin compaction into micro-tissues, the micro-tissues were cultured with one post held for one day to increase the effective stiffness, after which the magnet was removed to decrease the effective stiffness in real time (Supplementary Video-1).

To create a more drastic reduction in the ability of the cells to generate forces, we fully released the micro-tissues from one of the posts, as shown in Figure 3, after two days of culture while suspended between two posts. VICs were pretreated either with 10% FBS and 5 ng/mL TGF-β-1 or with 1% FBS and no TGF-β1 for four days and then cast in fibrin gels.

The micro-tissues were cultured for two days in their respective media before complete release of the boundaries.

2.5 Evaluating α-SMA and Apoptosis

To visualize α-SMA, tissues were blocked with 1.5% normal goat serum in PBS for 30 minutes, and then incubated with primary anti-α-SMA (Sigma, St. Louis, MO) antibody for 1 h. Fluorescently labeled secondary antibody (AlexaFluor-546, Invitrogen, Carlsbad, CA) was then applied, followed by imaging with a Leica SP5 point scanning confocal/DMI6000 inverted microscope. Fixed mouse brain and rat carotid tissues were stained in parallel as negative and positive controls, respectively.

To detect apoptotic cells, 5μM NucView 488 Caspase-3 assay substrate (Biotium, Hayward, CA) was applied to micro-tissues for 30 minutes prior to fixing the tissues. This assay substrate consists of a fluorogenic DNA dye coupled to the caspase-3/7 DEVD recognition sequence, which is initially non-fluorescent; when caspase-3/7 cleaves the substrate in apoptotic cells, a high-affinity DNA dye with bright green fluorescence is released. As a positive control for caspase-3 expression, 5 μM staurosporin was applied to micro-tissues for 5 hours in a separate dish. Micro-tissues were fixed in 4% paraformaldehyde and permeabilized with 0.25% Triton X-100 (Sigma, St. Louis, MO), stained, and analyzed using imaging microscopy. The total number of nuclei and the total number of apoptotic cells were counted in each micro-tissue.

2.6 Statistical Analysis

All data points are reported as mean ± standard deviation. Statistical comparisons were made using either t-test or two-way analysis of variance (ANOVA) depending upon the number of groups, with $p < 0.05$ considered significant. When a significant difference was found with two-way ANOVA, pairwise comparisons were completed with the Holm-Sidak method (Sigmaplot 11.0, Systat Software, San Jose, CA).

3. Results

3.1 Effects of Changing Boundary Stiffness in Real Time on Cell-Generated Forces

Based on our previous findings utilizing multiple combinations of boundary (post) stiffness and TGF-β1 concentrations [15], we chose a post stiffness level for which we predicted a two-fold change in stiffness that would have a substantial effect on cell-generated forces. With medium soft boundaries (k_{eff} = 0.165 nN/nm), the cell-generated forces increase for approximately two days, then level off at a homeostatic level of tension. In contrast, when one post is held rigidly by placing the magnet close to the culture dish (k_{eff} = 0.33 nN/nm), the stretch upon application of the magnet has a small magnitude (∼4%) and results in only a small initial increase in force <1 μN), yet cell-generated forces start to increase rapidly and continue to increase until the magnet is removed. When the magnet is removed, the tissue tension drops abruptly to 65-87% of the peak force value, but then begins to steadily increase. In the stiffened/softened group (stiffened to k_{eff} = 0.33 nN/nm and softened back to k_{eff} = 0.165 nN/nm in real time), the cell-generated forces rebound to the peak values within two days of additional culture (Figure 4A). While the force-per-cell values were different in

individual tissues, which caused high deviations, each individual tissue tension kept increasing following the reduction in boundary stiffness (Figure 4B).

3.2 Effect of Boundary Stiffness Reduction on α-SMA Distribution

No change in the α-SMA distribution was observed as a result of changing the boundary stiffness in real time by removing the magnetic force (Figure 5), unless the micro-tissue was entirely released from one post. All of the cells incorporate α-SMA into stress fibers, both on the outer surface and inner regions of dog bone-shaped tissues (Supplementary Videos 3 and 4). In contrast, no α-SMA-positive cells were observed in the core of the balled-up tissues that were completely released from one post (Figure 6). The cells on the outer surface of these retracted tissues stained positive for α-SMA, indicating the persistence of the myofibroblast phenotype in the cells covering the micro-tissues.

3.3 Effect of Boundary Stiffness Reduction on Apoptosis

Apoptosis was observed only when VICs were pretreated with 5 ng/ml TGF-β1 before seeding into the micro-tissues. The proportion of apoptotic cells is relatively low (<6%) and does not increase significantly when the effective boundary stiffness is reduced by releasing the rigidly held post (5.7% ± 2.04% caspase-positive cells in real-time stiffened/softened group vs. 4.07% ± 2.67% in the continuously soft group, $p>0.05$) (Figure 7). The tension drop was relatively small upon release of the magnet (from ∼0.9 μN/cell to 0.7 μN/cell). Releasing micro-tissues from posts completely and letting them contract into a ball increases the proportion of apoptotic cells significantly (31.4 ± 21.1%). Apoptosis did not significantly increase either when tissues were not released completely (Figure 6 C and D) or when cells were pre-treated and cultured with low serum prior to release (1% FBS) (Figure 6 and 8).

4. Discussion

This study is the first quantitative investigation of the effects of dynamic changes in stiffness on cell behavior within extracellular matrix. As expected based on our previous work, higher boundary stiffness resulted in increased cell-generated forces indicating a more highly activated myofibroblastic phenotype, which was not reversed upon removal of the magnet as evidenced by persistent α-SMA positive stress fibers and increasing cell-generated forces. As myofibroblasts are known to aggressively remodel ECM, we hypothesize that the continued rise in forces, even upon removal of the magnet, is due to the enhanced organization of the ECM and to concomitant local stiffening. Our preliminary matrix modulus measurements suggest that local stiffening does occur, but the analysis is not conclusive at this time. In contrast, when tissues were entirely released from one post to minimize the ability of the cells to generate tension, the proportion of apoptotic cells increased more than five-fold, and α-SMA staining was abrogated in the central region. Together, these data indicate that an increase in boundary stiffness, even if modest and temporary, can have lasting effects on myofibroblast persistence in tissues, and that a large decrease in the ability of the cells to generate tension is required to trigger dedifferentiation and apoptosis.

4.1 Increased boundary stiffness induces sustained increases in cell-generated force

In contrast to the continued rise in tension observed in our 3D micro-tissues, when single isolated cells cultured on a micro-post array are stretched, the traction forces increase for only approximately 20 minutes, then decrease to baseline over the next 40 minutes [25]. Similarly, when single isolated cells are cultured on collagen gels and stretched, the cell traction force increases but then returns to baseline within eight minutes of release for 5.5% substrate strain and decreases below baseline for 11% strain [26]. Further, upon release from relatively short duration stretch (4- or 30-second hold time), Fredberg and colleagues [27] observed a precipitous decrease in cell tension for cells cultured on polyacrylamide gels, after which the cell traction recovered over approximately 30 minutes (for homogeneous stretch).

Application of the magnetic force caused only a slight increase in tissue tension (quantified by deflection on the post without the magnetic beads), due to the small strain applied and the low modulus of the micro-tissues after only one day of culture. The average tissue stiffness before application of the magnet was ∼0.08 N/m, which indicates that the tissues are very soft at this early time point. Thus, we attribute the change in force following application of the magnet to increased cell-generated forces acting against the increased boundary stiffness. Positive feedback due to local stiffening may also, in part, promote sustained increases in contractile forces in the 3D micro-tissues. Recently, using the same μ-TUG system, Zhao et al. [29] showed that the modulus of the micro-tissues correlates positively with the stiffness of the posts that support the tissues, and this trend was observed for our tissues as well (Supplementary Fig. 6 and Video 2). In the aforementioned 2D systems, this dynamic reciprocity between the cells and matrix does not exist, which may explain the relatively rapid attenuation of force.

4.2 Persistence of α-SMA incorporation in stress fibers

Anseth and colleagues observed a decrease in α-SMA-positive staining of VICs upon reduction of a 2D substrate modulus from 32 kPa to 7 kPa after three days of culture and interpreted this finding as mechanically induced dedifferentiation [33]. We did not observe any change in α-SMA incorporation into stress fibers in the micro-tissues upon release of the magnetic force (see Supplemental Videos 3 and 4), possibly due to a shorter culture period at the high stiffness level (24 hrs) and/or insufficient change in tension (effectively by half). To decrease the boundary stiffness more drastically, we completely released micro-tissues from one post after 2 days of culture and found no α-SMA+ cells in the inner regions of the balled-up tissues where the tension is likely to be very low. We did observe substantial α-SMA incorporation in stress fibers on the tissue surface on which the tension is relatively high due to the geometric constraints. These data may indicate that there is a dose-dependent limit of lineage plasticity for the myofibroblast-to-fibroblast transition. There also may be a time limit of plasticity, as in a more recent study, Anseth and colleagues did not observed a phenotypic shift upon a decrease in substrate modulus after seven days of culture of VICs on a stiff substrate [22].

In contrast to findings from previous studies of micro-tissues cultured between compliant posts [15, 29], we observed α-SMA incorporation in the stress fibers of the cells both on the

surface and within the dog bone-shaped tissues (Supplementary Videos 3 and 4). In our previous study in which cells were not treated with TGF-β1 prior to seeding into micro-tissues, only the cells on the surface of the micro-tissues expressed α-SMA+ stress fibers (Supplementary Videos 5 and 6). Cells pretreated with TGF-β1 during 2D culture appear to preserve α-SMA in their stress fibers even after seeding into fibrin micro-tissues, in agreement with previous findings on myofibroblast memory [28].

4.3 Mechanical induction of apoptosis

Several studies have reported that apoptosis is induced by releasing rigidly anchored myofibroblast-populated collagen gels and letting them freely contract and by removing rigid splints holding wound edges [17-19]. Mathematical analysis by Humphrey and colleagues indicates that the stress in the center regions of free-floating fibroblast-populated collagen gels is very low, yet substantial stresses can remain at the edges after active contractile remodeling [34]. A rough correlation between the severity of the tension drop and the proportion of apoptotic cells appears to be emergent. In order of increasing severity of tension drop (estimated but not quantified), releasing a splinted wound likely reduces the tension from a high level to a moderate level and results in 8% apoptosis [17], completely releasing myofibroblast-populated collagen gels from high tension to very low (zero boundary stiffness) results in 15% apoptosis [18], and completely releasing scar myofibroblast-populated collagen gels from very high tension to low (zero boundary stiffness) results in 40% apoptosis [19]. In good agreement with these studies, we found that a large drop in tension (from 13 μN to zero) with complete release of TGF-β-pretreated cells results in substantial apoptosis (39%), whereas small changes (from 4 μN to zero) in tension upon complete release of non-TGF-β-pretreated tissues and with the halving of boundary stiffness do not induce apoptosis.

5. Conclusion

The results of this study demonstrate that with only a temporary increase in boundary stiffness, cell-generated forces continue to increase as if the stiffness had not been reduced back to its relatively soft baseline value. The reasons for the continued high generation of force-per-cell are unclear at this time. The lack of phenotypic reversion upon decrease in stiffness could be due to increased cell density or cell-cell contact with increased compaction while the posts were being held, or possibly due to an increase in intrinsic stiffness of the ECM due to enhanced remodeling during the time that the post was held magnetically. Extensive experiments are planned to induce contractile pathways, inhibit cell-cell communication, and block ECM secretion and crosslinking to further investigate these potential mechanisms.

Here, we also demonstrate that the extend of tension reduction plays an important role in myofibroblast persistence and apoptosis. The myofibroblast phenotype was shown to be persistent (at least on the outer surface of the micro-tissues) regardless of the drop in tension, and apoptosis was observed only with TGF-β1 pretreatment, which resulted in a high initial force and thus a large drop in tension. These findings imply that it is very difficult to de-activate the myofibroblast phenotype by mechanical means once it reaches a certain severity, without fully collapsing the tissue engineered structures. To prevent the

development of this irreversible situation, cell-generated forces and cell phenotype may need to be regulated throughout the entire *in vitro* culture period during development of engineered connective tissue substitutes by careful control of the mechanical environment and selection of media components. Preventing excessive myofibroblast activation and tissue stiffening could be an important strategy in the creation of functional tissue equivalents without fibrocontractive remodeling.

Supplementary Material

Refer to Web version on PubMed Central for supplementary material.

Acknowledgments

The authors gratefully thank the Chen Lab (University of Pennsylvania) for providing the μ-TUG stamps. The authors also thank Victoria Huntress for her help with confocal microscopy, Hans Snyder for his guidance in histology, and Ngozi Eze for proofreading. We acknowledge support from the National Institutes of Health (1R15HL087257-01A2) and the U.S. Army Medical Research and Materiel Command (W81XWH-11-1-0631).

References

1. Hinz B. Formation and function of the myofibroblast during tissue repair. J Invest Dermatol. 2007; 127(3):526–37. [PubMed: 17299435]
2. Desmouliere A, et al. Transforming growth factor-beta 1 induces alpha-smooth muscle actin expression in granulation tissue myofibroblasts and in quiescent and growing cultured fibroblasts. J Cell Biol. 1993; 122(1):103–11. [PubMed: 8314838]
3. Hinz B, et al. The myofibroblast: one function, multiple origins. Am J Pathol. 2007; 170(6):1807–16. [PubMed: 17525249]
4. Tomasek JJ, et al. Myofibroblasts and mechano-regulation of connective tissue remodelling. Nat Rev Mol Cell Biol. 2002; 3(5):349–63. [PubMed: 11988769]
5. Sarrazy V, et al. Mechanisms of pathological scarring: role of myofibroblasts and current developments. Wound Repair Regen. 2011; 19(Suppl 1):s10–5. [PubMed: 21793960]
6. Henderson NC, Iredale JP. Liver fibrosis: cellular mechanisms of progression and resolution. Clin Sci. 2007; 112(5):265–280. [PubMed: 17261089]
7. Dussaule JC, et al. The role of cell plasticity in progression and reversal of renal fibrosis. Int J Exp Pathol. 2011; 92(3):151–7. [PubMed: 21314743]
8. Wallach-Dayan SB, Golan-Gerstl R, Breuer R. Evasion of myofibroblasts from immune surveillance: a mechanism for tissue fibrosis. Proc Natl Acad Sci USA. 2007; 104(51):20460–5. [PubMed: 18077384]
9. Mohler ER 3rd, et al. Bone formation and inflammation in cardiac valves. Circulation. 2001; 103(11):1522–8. [PubMed: 11257079]
10. Syedain ZH, et al. Implantation of a tissue-engineered heart valve from human fibroblasts exhibiting short term function in the sheep pulmonary artery. Cardiovasc Eng Technol. 2011; 2(2): 101–112.
11. Schmidt D, et al. Minimally-invasive implantation of living tissue engineered heart valves: a comprehensive approach from autologous vascular cells to stem cells. J Am Coll Cardiol. 2010; 56(6):510–20. [PubMed: 20670763]
12. Hinz B. Tissue stiffness, latent TGF-beta1 activation, and mechanical signal transduction: implications for the pathogenesis and treatment of fibrosis. Curr Rheumatol Rep. 2009; 11(2):120–6. [PubMed: 19296884]
13. Quinlan AM, Billiar KL. Investigating the role of substrate stiffness in the persistence of valvular interstitial cell activation. J Biomed Mater Res A. 2012; 100(9):2474–2482. [PubMed: 22581728]

14. Walker GA, et al. Valvular myofibroblast activation by transforming growth factor-beta: implications for pathological extracellular matrix remodeling in heart valve disease. Circ Res. 2004; 95(3):253–60. [PubMed: 15217906]
15. Kural MH, Billiar KL. Mechanoregulation of valvular interstitial cell phenotype in the third dimension. Biomaterials. 2014; 35(4):1128–37. [PubMed: 24210873]
16. Desmouliere A, et al. Apoptosis mediates the decrease in cellularity during the transition between granulation tissue and scar. Am J Pathol. 1995; 146(1):56–66. [PubMed: 7856739]
17. Carlson MA, Longaker MT, Thompson JS. Wound splinting regulates granulation tissue survival. J Surg Res. 2003; 110(1):304–9. [PubMed: 12697415]
18. Grinnell F, et al. Release of mechanical tension triggers apoptosis of human fibroblasts in a model of regressing granulation tissue. Exp Cell Res. 1999; 248(2):608–619. [PubMed: 10222153]
19. Linge C, et al. Hypertrophic scar cells fail to undergo a form of apoptosis specific to contractile collagen-the role of tissue transglutaminase. J Invest Dermatol. 2005; 125(1):72–82. [PubMed: 15982305]
20. Wipff PJ, et al. Myofibroblast contraction activates latent TGF-beta1 from the extracellular matrix. J Cell Biol. 2007; 179(6):1311–23. [PubMed: 18086923]
21. Wang H, et al. Redirecting valvular myofibroblasts into dormant fibroblasts through light-mediated reduction in substrate modulus. PLoS ONE. 2012; 7(7):e39969. [PubMed: 22808079]
22. Wang H, et al. Hydrogels preserve native phenotypes of valvular fibroblasts through an elasticity-regulated PI3K/AKT pathway. Proc Natl Acad Sci USA. 2013
23. Quinlan AMT, et al. Combining dynamic stretch and tunable stiffness to probe cell mechanobiology in vitro. PLoS ONE. 2011; 6(8):e23272. [PubMed: 21858051]
24. Sander EA, Barocas VH, Tranquillo RT. Initial Fiber Alignment Pattern Alters Extracellular Matrix Synthesis in Fibroblast Populated Fibrin Gel Cruciforms and Correlates with Predicted Tension. Annals of biomedical engineering. 2011; 39(2):714–729. [PubMed: 21046467]
25. Mann JM, et al. A silicone-based stretchable micropost array membrane for monitoring live-cell subcellular cytoskeletal response. Lab Chip. 2012; 12(4):731–40. [PubMed: 22193351]
26. Gavara N, et al. Mapping cell-matrix stresses during stretch reveals inelastic reorganization of the cytoskeleton. Biophys J. 2008; 95(1):464–71. [PubMed: 18359792]
27. Krishnan R, et al. Reinforcement versus fluidization in cytoskeletal mechanoresponsiveness. PLoS One. 2009; 4(5):e5486. [PubMed: 19424501]
28. Balestrini JL, et al. The mechanical memory of lung myofibroblasts. Integr Biol (Camb). 2012; 4(4):410–21. [PubMed: 22410748]
29. Zhao R, Chen CS, Reich DH. Force-driven evolution of mesoscale structure in engineered 3D microtissues and the modulation of tissue stiffening. Biomaterials. 2014; 35(19):5056–64. [PubMed: 24630092]
30. Goffin JM, et al. Focal adhesion size controls tension-dependent recruitment of alpha-smooth muscle actin to stress fibers. J Cell Biol. 2006; 172(2):259–68. [PubMed: 16401722]
31. Hinz B, Gabbiani G. Cell-matrix and cell-cell contacts of myofibroblasts: role in connective tissue remodeling. Thromb Haemost. 2003; 90(6):993–1002. [PubMed: 14652629]
32. Verhoekx JS, et al. Isometric contraction of Dupuytren's myofibroblasts is inhibited by blocking intercellular junctions. J Invest Dermatol. 2013; 133(12):2664–71. [PubMed: 23652794]
33. Kloxin AM, Benton JA, Anseth KS. In situ elasticity modulation with dynamic substrates to direct cell phenotype. Biomaterials. 2010; 31(1):1–8. [PubMed: 19788947]
34. Simon DD, Horgan CO, Humphrey JD. Mechanical restrictions on biological responses by adherent cells within collagen gels. J Mech Behav Biomed Mater. 2012; 14:216–226. [PubMed: 23022259]
35. Niland S, et al. Contraction-dependent apoptosis of normal dermal fibroblasts. J Investig Dermatol. 2001; 116(5):686–692. [PubMed: 11348456]
36. Miyakoshi J. Effects of static magnetic fields at the cellular level. Prog Biophys Mol Biol. 2005; 87(2–3):213–223. [PubMed: 15556660]

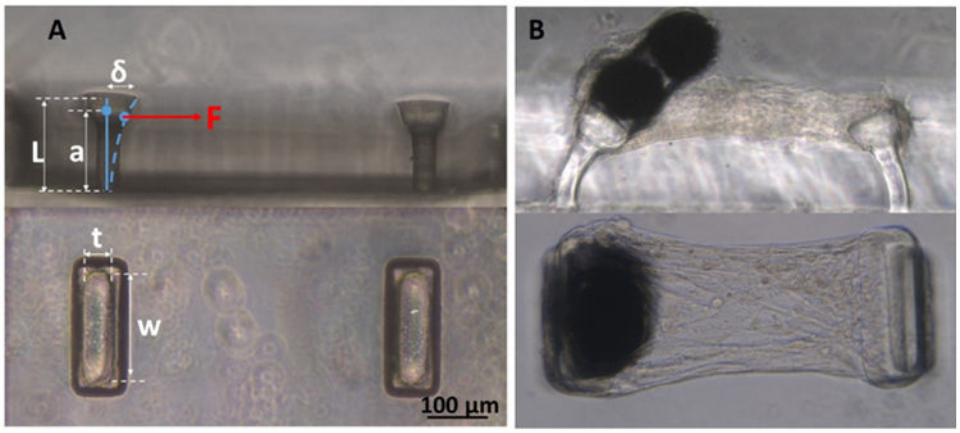

Figure 1.
Micro-tissue gauges (μ-TUGs). A: Side and top views of an empty μ-TUG well. B: Side and top views of a micro-tissue with magnetic beads glued on top of one of the micro-posts.

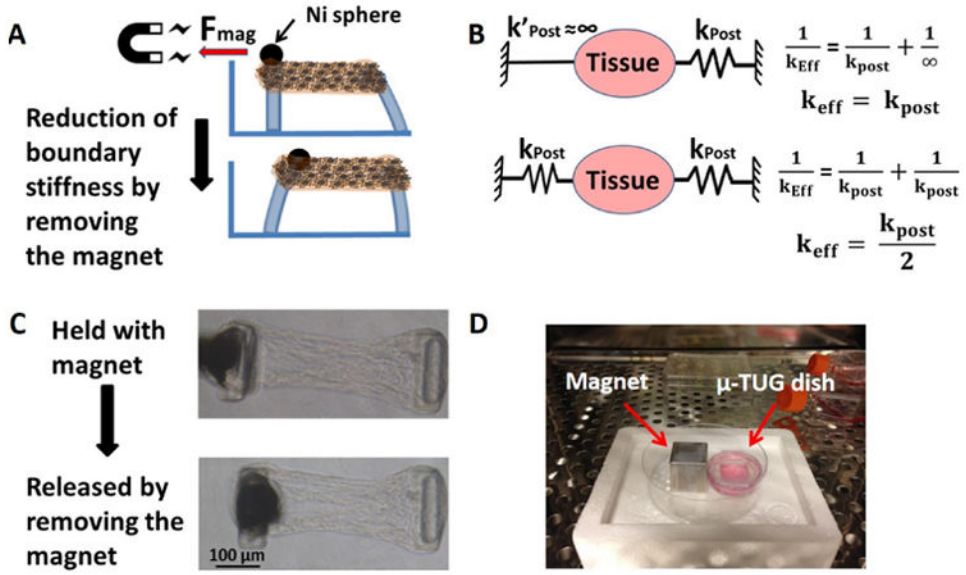

Figure 2.

A: Nickel particle glued onto the micro-post is held rigidly by a permanent magnet for one or two days. Stiffness is reduced in real time by removing the magnet. B: Calculation of estimated effective boundary stiffness as a result of holding one of the posts. C: A μ-TUG dish with permanent magnet in the incubator. D: Phase images of micro-tissue before and after removing the magnet.

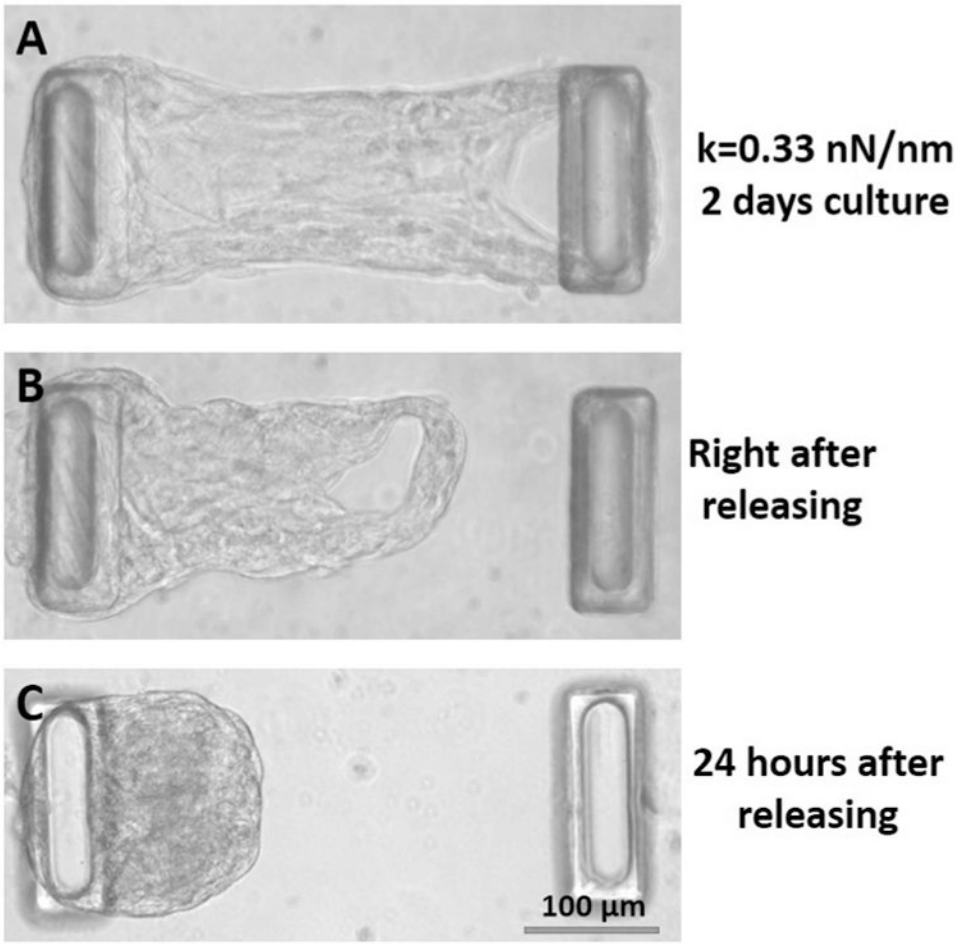

Figure 3.
Phase images of attached and fully-released micro-tissues. A: Before release (two days of culture). B: Immediately after releasing the tissue. C: 24 hours after release.

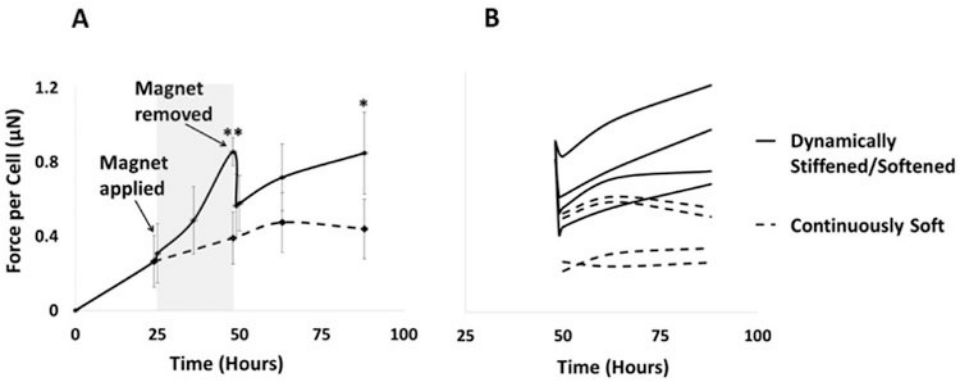

Figure 4.

Cell-generated force response to real-time changes in boundary stiffness. A: Average force per cell over time for k_{eff} = 0.165 nN/nm for both groups initially; in the real-time stiffened/softened group, k_{eff} increases to 0.33 nN/nm by application of magnetic force (grey region) at hour 26 and decreases back to 0.165 nN/nm upon removal of the magnet at hour 50 (blue region on the right). For all samples, cells were pretreated with 10% FBS and 5 ng/mL TGF-β1 before forming micro-tissues, and 10% FBS and 1 ng/ml TGF-β1 were used during the micro-tissue culture period. Holding one post rigidly increased cell-generated forces. Removal of the magnet caused an abrupt drop in tissue tension, but the tension rebounded and continued to increase following removal of the magnet for all of the dynamically stiffened samples. (T-test: * $p<0.05$, **: $p=0.001$). B: Change in force per cell in each individual micro-tissue after removal of the magnet demonstrates a continuous increase in tension for all dynamically stiffened micro-tissues.

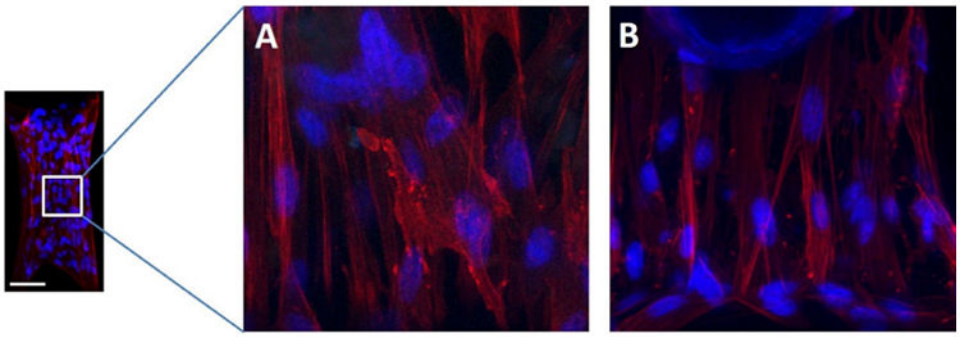

Figure 5.

A: Immunofluorescent staining in a micro-tissue with one post held rigidly (higher boundary stiffness) after 48 hours of culture (24 hours after introducing the magnet) (α-SMA (red) and cell nuclei (blue)). B: The same staining for a micro-tissue held in a continuously soft (lower boundary stiffness) configuration after 48 hours of culture. The sequestration of α-SMA into the stress fibers in these images indicates that the VICs in both groups are myofibroblasts. No consistent trends in cell alignment or nuclear aspect ratio were observed. In each group, cells were pretreated with 10% FBS and 5 ng/mL TGF-β1 for four days before forming micro-tissues, and 10% FBS and 1 ng/ml TGF-β1 were used during culture of the micro-tissues. The individual post stiffness = 0.33 nN/nm. Scale bar: 100 μm.

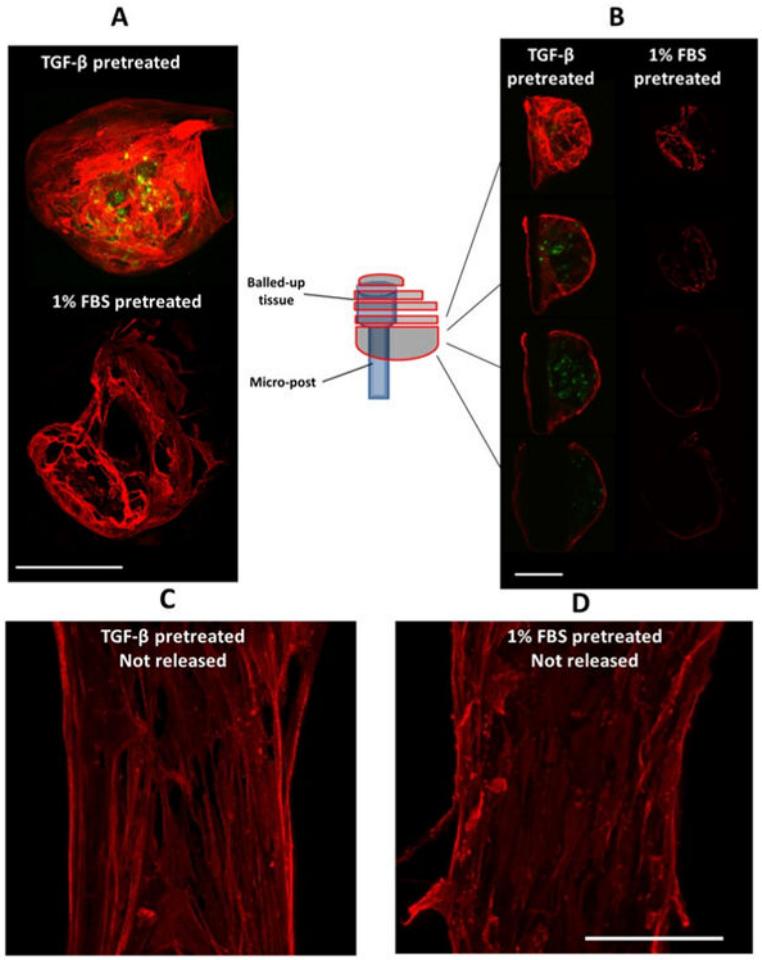

Figure 6.

A: Maximum projections of confocal images of a fully released micro-tissue two days after release (α-SMA (red); caspase-3 (green)). VICs were pretreated either with 10% FBS and 5 ng/mL TGF-β1 or with 1% FBS and no TGF-β1 for four days and then seeded into micro-tissues. The micro-tissues were cultured for two days in their respective media before complete release of the boundaries. The samples were probed for caspase-3 (apoptosis marker) two days after release. B: Z-stack slices at different levels of the micro-tissues. Only cells on the surface of the (balled-up) tissues completely released from one post stained positive for α-SMA, while only the cells in the inner regions of TGF-β1 pretreated group stained positive for the apoptotic marker. Maximum projections of confocal images of micro-tissues that are not released C: TGF-β1 pretreated and D: 1% FBS pretreated (scale bars: 100 μm).

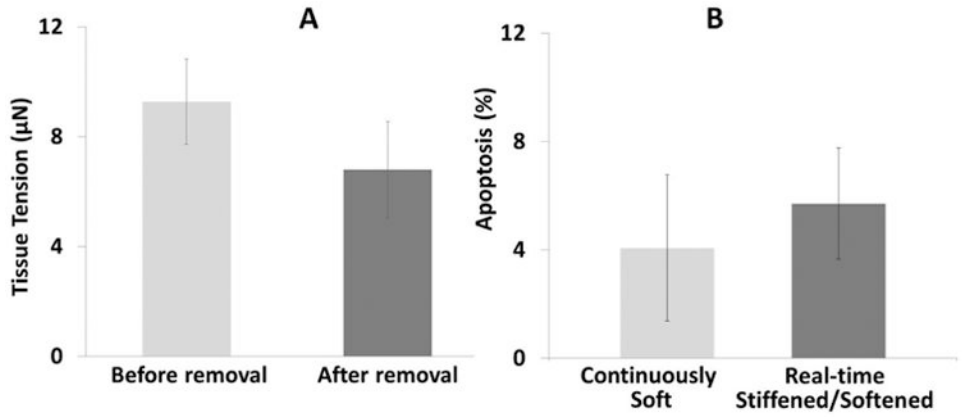

Figure 7.

Effect of dynamic softening by removal of the magnet on cell-generated tension and apoptosis. A: Tissue tension after 24 hours of culture decreases following removal of the magnet (n.s.). B: The % apoptosis (measured by caspase-3 staining) in the Real-time Stiffened/Softened group two days following reduction in the boundary stiffness back to the baseline level was not significantly higher than in the Continuously Soft group. For both groups, cells were pre-treated for four days with 10% FBS and 5 ng/mL TGF-β1 before seeding into the fibrin gels and cultured in the same media for culture of the micro-tissues; the individual post stiffness = 0.33 nN/nm. For the Real-time Stiffened/Softened group, a magnet was applied for 24 hours then removed, whereas no magnet was applied for the Continuously Soft group.

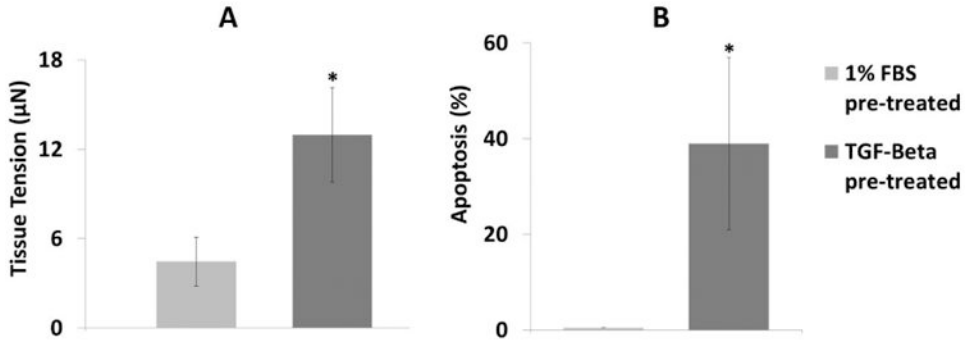

Figure 8.

A: There was significantly higher tension in the TGF-β–pretreated group than in the low FBS-pretreated group after two days of culture. B: The proportion of cells that stained positive for apoptosis in the fully-released tissues was significantly higher with TGF-β1 pre-treatment than with low FBS two days after release (n=3, *: $p<0.05$, t-test). These micro-tissues were cultured for two days then released, and caspase-3 levels were measured after an additional two days of culture in the released state. Cells were either pre-treated with 1% FBS without TGF-β1 or 10% FBS with 5 ng/mL TGF-β1 for four days before seeding into the fibrin gels.